# Fourth Workshop on Non-Linear Dynamics and Earthquake Prediction

## 6 - 24 October 1997

# *Quantitative Seismology and Rockmass Stability*

*A. MENDECKI*

ISS International
PO Box 2083, 9460 Welkom,
SOUTH AFRICA

# PRINCIPLES OF MONITORING
# SEISMIC ROCKMASS RESPONSE TO MINING

by

### Aleksander J Mendecki

*ISS International, PO Box 2083, Welkom, 9460 South Africa,*
alexm@frg.issi.co.za

ABSTRACT: Today, technology and techniques of monitoring seismic rockmass response to mining allow one to quantitatively analyse hundreds of seismic events, with 'well-behaved' waveforms, per shift and to quantify seismicity by parameters relating to change in strain, stress or rheology of seismic deformation. It is proposed that the imminence of potential rockmass instability be quantified by a time-to-failure model with observable rate dependent seismic parameters to increase the sensitivity to precursory behaviour. It is suggested that a system be developed for continuous – in addition to intermittent – monitoring of rockmass response to mining, where sensors are positioned at the centre of the seismically active area as opposed to being outside in the far field. Nonlinear time series analysis would allow the classification of the underlying dynamics, build the predictive models and, hopefully, facilitate the controlled manipulation of the rockmass response to mining into desirable states of stability or instability.

## 1. INTRODUCTION

Mining excavations induce elastic and then inelastic deformation within the surrounding rock. The potential energy accumulated during elastic deformation may be unloaded or it may be released gradually or suddenly during the process of inelastic deformation. A seismic event is a sudden inelastic deformation within a given volume of rock i.e. seismic source, that radiates detectable seismic waves.

Seismic rockmass response to mining at a given site can then be characterised by its ground motions, due to sudden inelastic deformation and resulting seismic waves, measured above the average premining level.

Figure 1 shows the velocities of ground motion recorded at different sites in mines. From top to bottom:
- Noise of an average velocity of $10^{-6}$ m/s.
- Noise with a few emerging coherent structures at a level of $7 \cdot 10^{-6}$ m/s.
- A very small $m_M=-2.5$ well-behaved seismic event recorded by an accelerometer at a distance of 133 m from its source.
- A well-behaved and good quality waveform of a seismic event of magnitude $m_M=0.2$ recorded at a distance of 253 m from the source.
- Two seismic events or a double event of magnitude $m_M=2.1$ and 2.0, respectively, recorded at a distance of 185 m from the source.
- The same double seismic event as immediately above, recorded at a distance of 2586 m from the source.
- A seismic event $m_M=2.3$ recorded at a distance of 121 m from the source with, most likely, intermediate or even near-field components of seismic radiation.

A superficial inspection of the waveforms presented in Figure 1 would reveal certain recognisable deterministic patterns or coherent structures, in this case called seismic events, and the remaining ground motion would be classified as 'random', negligible noise.

Seismic events, as dissipative coherent structures, contain newly created information about the state of the system at and in the vicinity of their sources at the times of their occurrence.
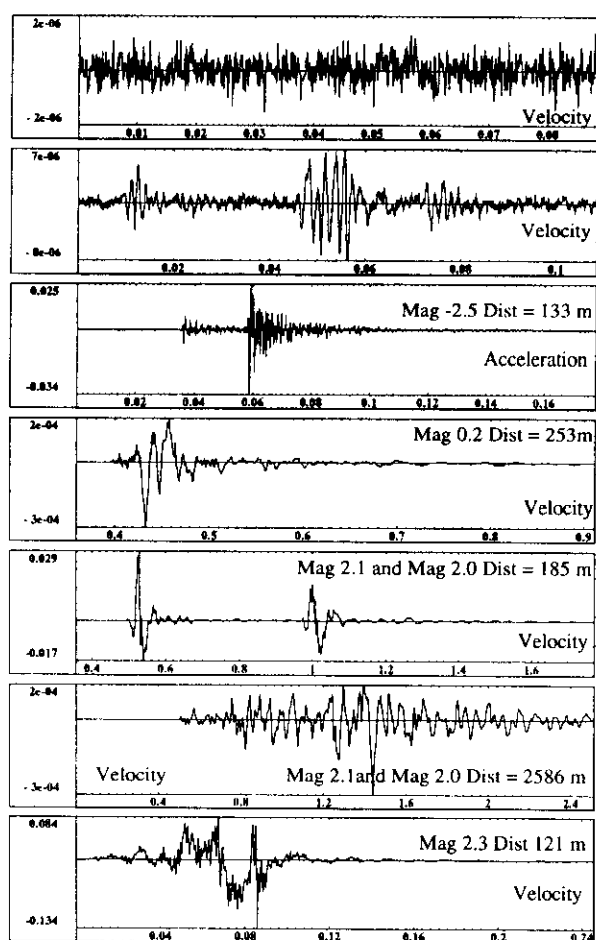


Figure 1 Selected waveforms of ground motion recorded in mines. The ground motion varies from an average of $10^{-6}$ m/s which could be characterised as low level noise, through convoluted motions at $7 \cdot 10^{-6}$ m/s level resulting from microfracturing and/or mining activity, to strong ground motion with a peak particle velocity of 0.13 m/s resulting in a seismic event of $m_M=2.3$, recorded 121 m from its source.

That information will become useful only once extracted and translated into parameters relevant to associated changes in stress and strain and/or into invariant characteristics of the dynamics of seismic rockmass response to mining, i.e. fractal dimensions and Lyapunov exponents.

In today's practice of quantitative seismology in mines, only waveforms of seismic events with certain characteristics, i.e. sufficient signal to noise ratio, low complexity of source, negligible near- or intermediate terms of source radiation, weak site effects, are being processed routinely. These requirements unavoidably limit the amount of seismic information available about the state of the rockmass.

If sufficient numbers of three-component seismic stations, say at least five, surrounding the event record such 'quality' waveforms then, apart from its time and location X=(xyz), one can reliably calculate at least two independent parameters pertaining to its source, namely seismic moment $M$ including its tensor $M_{ij}$, radiated seismic energy $E$ or seismic moment and stress drop $\Delta\sigma$.

Having recorded and processed a number of seismic events within a given volume of interest $\Delta V$ over time $\Delta t$, one can then quantify the changes in the strain and stress regime and in the rheological properties of the rockmass deformation associated with the seismic radiation. In turn, that facilitates the following objectives of quantitative monitoring of seismic rockmass response to mining:

*   to verify assumptions of the design process to enable its continuity while mining and to promote controlled mining operations;
*   to predict potential instabilities of the underground structures to save lives; and
*   to back analyse to improve the efficiency of both the design and the monitoring process.

This paper describes requirements and possible solutions to the problems encountered in achieving these objectives. Since seismic monitoring involves: sensors, data acquisition with its central site, seismological processing and analysis software, the paper is structured accordingly. In conclusion, I speculate on future research and development needs. Seismic site effects at the skin of the excavation and damage mechanisms are not considered in this paper.

## 2. SEISMIC MONITORING SYSTEMS

A seismic system consists of transducers, a central processing site, and a means of communication between the two.

### 2.1 Transducers

Inertial seismic sensors may be characterised by the ranges of frequency and amplitude of ground motion which can be reliably converted to an electrical signal.

Seismic event spectra may be characterised by a corner frequency $f_0$ at which most energy is radiated. In order to quantify an event, frequencies from $f_0/2$ to $5f_0$ must be recorded for analysis. Corner frequency as a function of seismic moment is plotted in Figure 2, for several stress drops and a range of rock types.

Ground motion amplitudes at the sensor are not only dependent on the seismic source parameters, but also on the distance from the event and the seismic wave propagation
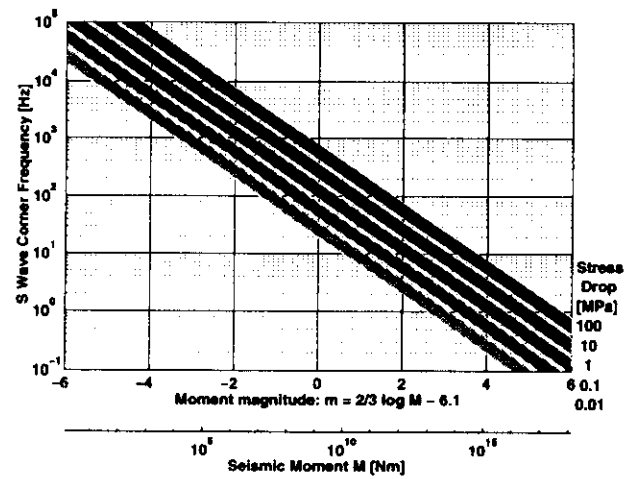


Figure 2 Expected S wave corner frequencies, $f_0$, as a function of seismic moment, $M$, for a range of stress drops, $\Delta\sigma$. The general relation is given by:

$$f_0 = \frac{KV_s}{2\pi}\sqrt[3]{\frac{16\Delta\sigma}{7M}}$$

where $K$ is a model dependent term, and $V_s$ is the S wave propagation velocity. A value of $K = 2.34$ from the Brune model is illustrated. The width of each band shows the variation with $V_s$ from 2000m/s, typical of soft rock, to 3700m/s, for hard rock.
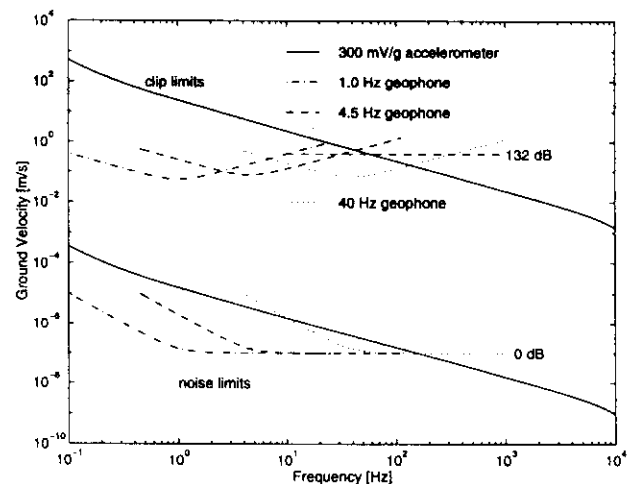


Figure 3 Sensitivity and dynamic range of sensors commonly used in mine seismic systems. The region between the noise and clip limits represents the usable range for each instrument. The noise limit is represented by the broadband noise level as measured by a long term average (LTA), rather than noise spectral density. The geophone's greater sensitivity up to several hundred Hz is clearly shown, as is the loss of dynamic range due to displacement clipping below these frequencies. A data acquisition system dynamic range of 132 dB with its quantization noise matching the expected ground noise of $10^{-7}$ m/s is illustrated (after Mountfort and Mendecki, 1997).

characteristics, which leads to the need for an extremely wide dynamic range in amplitude. For reasons of economy, the sensors used in mine monitoring systems are usually either miniature geophones or piezo-electric accelerometers. Figure 3 shows the ranges of amplitude, in terms of ground velocity,
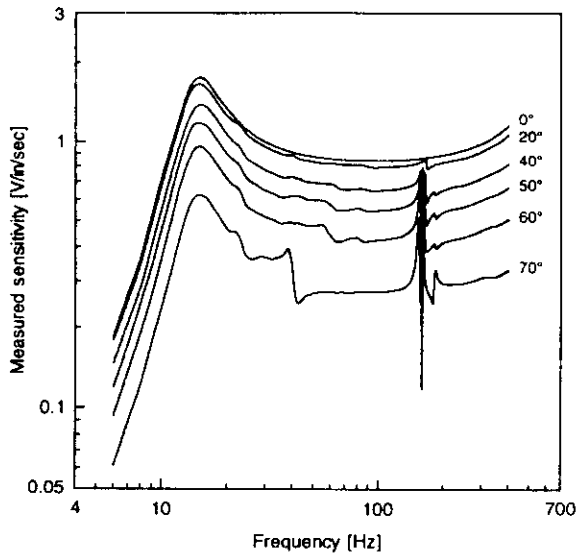
Figure 4 Variation in geophone sensitivity with angle of excitation. The average sensitivity, as expected, varies as the cosine of the excitation angle (0°=axial, 90°=radial), but the transverse modes can produce almost the full response at a certain frequency even at a large angle. This figure was produced using a 14 Hz geophone. Reproduced from Oh (1996).
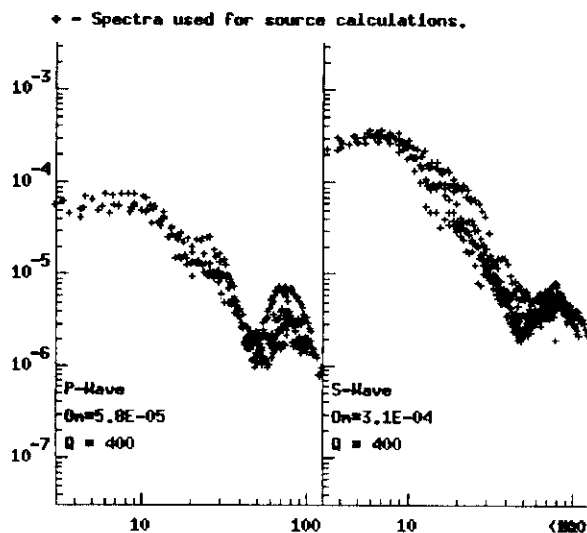


Figure 5 Distance and Q corrected displacement spectra of a seismic event recorded by 6 stations with clearly visible 'spurious' frequencies, most likely an artifact of geophone radial response.

which may be measured by typical devices, as a function of frequency.

Geophones, by virtue of operating above their natural frequency $f_n$, are inherently sensitive devices. Real geophones have a relatively narrow useful frequency range, bounded at the lower end by $f_n$ and at the upper by the lowest 'spurious' frequency, denoted $f_{cl}$ for clean bandwidth. Spurious frequencies are resonances excited by off-axis motion, as illustrated in

Figure 4 and Figure 5. Because these resonances are an artifact of the mechanical construction, a useful figure of merit for geophones is the ratio $f_{cl}/f_n$, which may approach 40 in the best cases. This compares with a factor of ten required to measure events with a single $f_0$. The fall off in sensitivity below $f_n$, and related phase shift, adheres closely to the theoretical model and may be deconvolved to extend the usable bandwidth to lower frequencies by at least a factor of two.

While geophones do have a good dynamic range, approaching 120 dB at $f_n$ above even the high environmental noise observed in mines, they do suffer from clipping and should not be used in the near field of events m>1. Because this clipping is due to limited displacement and the output is proportional to ground velocity, it is not immediately apparent on a seismogram. Accelerometers theoretically have a useful frequency range from $f_n$ down to zero. i.e. constant acceleration. The piezo-electric units have a very low damping factor, which means that the highest usable frequency is about $f_n/2$. There is always some charge leakage which sets a lower limit, but the ratio of lowest to highest usable frequency is nevertheless usually ~10000, a true broadband response. The tradeoff is lower sensitivity compared with geophones. Since the high frequencies which the accelerometers are capable of receiving also do not propagate well, accelerometers must be mounted close to the area of interest. The low frequency insensitivity is then an advantage, as there is little danger of clipping on nearby large events. Table 1 shows some application scenarios in terms of type and distribution of sensors.

For events with corner frequencies below 4 Hz (see Figure 2) the low cost sensors are inadequate and special purpose earthquake sensors are required, in the form of a 1 Hz geophone or a force balance accelerometer. If any large events are anticipated, at least one 3-component sensor per mine is required to provide accurate seismic moment estimates.

## 2.2 Data acquisition

The data acquisition system must record the amplitude and timing of ground motion at sensors distributed throughout the volume of interest and assemble the data at a central point for processing.

Generally the data are digitised as close to the sensor as possible, since in this form it is possible to protect against corruption. In mines, the results must be available within a reasonably short time, and different media are used for communication, including radio, copper twisted pair and optical fibre. Where the sensor bandwidth is matched by the information rate of the communication channel, ground motion data may be continuously transmitted to the central site for storage and sophisticated multipass processing. Often the communications bandwidth is insufficient, so the data must be reduced at site before transmission, and the time maintained locally at each sensor. Triggering, validation and data reduction processes may be used to select and preprocess data corresponding to valid seismograms for storage and later transmission. In this way the required communication bandwidth may be reduced by at least a factor of 100.

The central site should have sufficient resources for performing seismological processing, archival storage of event and waveform data, and assisting in interpretation by visualisation techniques.

| Application | Minimum system characteristics |
|---|---|
| Regional mining – monitoring of several operations on a regional basis, larger seismic events, $m_M \geq 0$, over relatively long distances (1 – 30 km) | Low Frequency: (1 Hz - 300 Hz)<br>Sensor density: 5 stations within 5 km of the source<br>Velocity Transducers: (Geophones)<br>Sampling rate: 500 Hz - 4 kHz<br>Event rate: 1 - 100 events per day<br>Communication rate: 1.2 kb/s<br>Communication method: single twisted pair and/or radio |
| Mine- or shaft-wide monitoring – from $m_M$ > -1 and distances from 300 m to 5 km | Medium frequency: (4.5 Hz - 2 kHz)<br>Sensor density: 5 stations within 1 km of the source<br>Transducers: Geophones/Accelerometers<br>Sampling rate: 10 kHz<br>Event rate: 100 - 1000 events per day<br>Communication rate: 115 kb/s<br>Communication method: dual twisted pair and/or optical fibre |
| Pillar/remnant monitoring from $m_M$ >-3 and distances from 100 m to 1 km | Medium frequency: (3 - 10 kHz)<br>Sensor density: 5 stations within 300 m from the source<br>Transducers: Accelerometers<br>Sampling rate: up to 50 kHz<br>Event rate: 1000 - 10 000 events per day<br>Communication rate: 19.2 kb/s with processing at site<br>Communication method: copper cable and/or optical fibre |
| Continuous quantification of seismic rockmass response to mining | High frequency: (3 - 15 kHz)<br>Sensor density: 3 - 6 components within 100 m radius<br>Transducers: Accelerometers<br>Sampling rate: 50 kHz<br>Event rate: continuous<br>Communication rate: 12 Mb/s or processing at site<br>Communication method: optical fibre |

Table 1. Application scenarios

## 3. SEISMOLOGICAL PROCESSING

### 3.1 Location of seismic events

Because of the logistical – "Where was it?" – and seismological importance of the location of seismic events in mines, it had, and to a certain extent still enjoys, the attention of researchers trying to improve the accuracy, objectivity and calculation time. Location error depends on the number and spatial distribution of seismic stations with respect to the position of the source and on the type and quality of the data. The following common sense and experience based comments are in order:

- For most routine applications the required accuracy for location is 2% to 3% of the average hypocentral distance from the source to stations used in the location procedure; trying to achieve better accuracy may prove costly. Errors over 5% are not acceptable.
- One needs a dense network of stations to maintain such an accuracy when P arrivals only and straight ray approximations are used in the location procedure; it is, however, the best solution for reliable automatic locations.
- While difficult to pick, S wave arrivals constrain the P based location process considerably and if supplemented by directions or azimuths from a few nearest stations it gives very reasonable results even in layered geological structures but with no major lateral inhomogenieties. This method is applicable for automatic locations but the success rate is compromised mainly by the accuracy of the S picks.
- In general, the application of a validation procedure that eliminates from processing waveforms which are unsuitable, see Figure 1 or, in some cases, undesirable, e.g. blasts, greatly improves the success rate of automatic location and

source parameter inversion. A backpropagation neural network (Cichocki and Umbehauen, 1993) has been tried with reasonable results (Mountfort and Mendecki, 1997).

- In cases of sparse and/or poorly configured networks employed within a complex, but known, geological structure one needs to apply a kinematic ray tracing procedure for reasonable locations, e.g. Vidale (1990); Qin et al. (1992); Cao and Greenhalgh (1994); Dzhafarov (1997b). One can precalculate the expected travel times for a dense grid and retrieve them during iterations to speed up calculations.
- In cases where the velocity model is not known adequately and/or if the velocity structure changes with time due to mining one can use a relative location technique if a master event, such as a blast, is available in the area of interest, e.g. Spence (1980); Poupinet et al. (1984); Gibowicz and Kijko (1994); Milev et al. (1995) or one can, having overdetermined observations, try to invert the location(s) and velocity model simultaneously, e.g. Mendecki (1987); Jech (1989); Maxwell and Young (1993) and (1997); Mendecki and Sciocatti (1997); both methods are rather difficult to implement in a routine automatic processing system.
- The interpretation of location, if accurate, depends on the nature of the rupture process at the source – if slow or weak rupture starts at a certain point, the closest station(s) may record waves radiated from that very point while others may only record waves generated later in the rupture process by a higher stress drop patch of the same source. One needs to be specific in determining the arrival times if the location of rupture initiation is sought, otherwise the location will be, as it is in most cases, a statistical average of, hopefully, different parts of the same source.

## 3.2 Seismic source parameters

Determination of source parameters, such as seismic moment, corner or predominant frequency and radiated seismic energy, has become routine for most mine seismic networks. It is a prerequisite if one wants to quantify seismic activity and compare or integrate results of stress modelling and seismic monitoring. Most of the employed schemes are based on a straight or slightly modified Brune's model that has proved extremely useful over the last 25 years, e.g. see Mendecki (1993), Spottiswoode (1993), Gibowicz and Kijko, (1994), Urbancic et al. (1996), and Mendecki and Niewiadomski (1997) for application to mine seismic networks. Yet frequently the same waveforms treated by different software packages yield different results. The following few comments may help in achieving more reliable and more consistent results:

- It is advisable to have waveforms from at least five three-component stations surrounding the source available for the inversions.

- Use of accelerometers, while highly desirable, is costly and involves double integration which may be implemented in either frequency or time domains. Integration of a time series is an inherently unstable procedure. Due to low gain at low frequency, noise might be amplified very strongly. It is therefore recommended that some prefiltering be used with the purpose of suppressing low frequency components (Dzhafarov, 1997a).

- Another problem experienced during spectral analysis is how to minimize the "energy leakage" which is caused by implicit windowing of data. Use of any one spectral taper, such as Hamming, Bartlett, etc, does not allow the desired spectral characteristics to be achieved. Application of a multitapering spectral estimation technique, which uses several specially designed windows may minimize the energy leakage problem, while producing the minimum variance spectral estimate. Each of these windows recovers information which has been lost by the previous windows, e.g. Park et al. (1987); Mendecki and Niewiadomski (1997).

- Processing of waveforms in the frequency domain permits easy inversion of, apart from seismic energy, the source dimensions and seismic moment, using the value of corner frequency and longwave asymptote of the displacement spectra. However, the frequency domain approach cannot be used for the parametrization of complex seismic sources, and information such as the source duration, shape and orientation cannot be determined in this manner. Time domain analysis of observed waveforms allows the construction of a source time function which reflects the heterogeneity of its mechanical properties, thus avoiding the a priori constraint of double couple mechanism, e.g. Niewiadomski, 1997. Further improvement can be obtained if the location of the source is allowed to vary in an a priori chosen range, e.g. Dziewonski and Woodhouse (1982); Šílený and Pšenčík (1995). Application of recently developed methods for the calculation of synthetic seismograms like recursive cell (Moser and Pajchel, 1996) and wavefront construction (Vinje et al., 1993; Dzhafarov, 1997b) raytracing methods can significantly speed up the inversion process.

- Problems with seismic source inversion are further complicated by nonlinearity of wave propagation, which causes every individual spectral component in a broadband signal to produce a second harmonic and a sum and
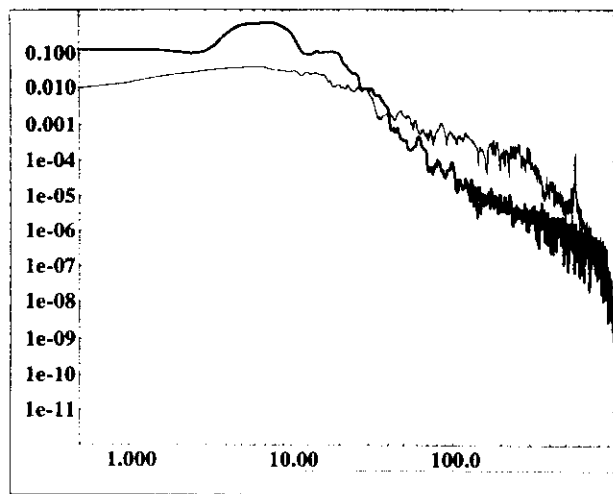


Figure 6 Displacement spectra of the S wave for a seismic event recorded by two stations which occurred on 6 January 1997. One station is situated close to the source (842m) and is shown as solid (dark) line, the other is distant (3230m). The seismograms have been deconvolved for the instrument response, corrected for geometrical spreading, and integrated to displacement prior to the application of a multitapering spectral estimation technique. An enrichment of the distant spectrum in high frequencies with distance is clearly visible in this case. Units on the vertical axis are in m/s; units on the horizontal axis are in Hz.

difference with every other component, expanding the original spectrum to both the low and high frequency ends. While it is very difficult to observe such nonlinear propagation effects at low frequency due to low resolution in this frequency range, it is observable in the high frequency range, causing misfit of the observed data to seismic source models based on a linear wave propagation assumption (Beresnev and Wen, 1996). Figure 6 shows the displacement spectra for S waves of a seismic event which occurred on 6 January 1997. One station is situated close to the source (842m) and is shown as solid line, another is a distant spectrum (3230m). The seismograms have been deconvolved for the instrument response and integrated to displacement prior to the application of a multitapering spectral estimation technique. An enrichment of the spectra in high frequency components, consistent with the results of theoretical modelling involving the nonlinear wave equation is clearly visible. Such nonlinear behaviour can be modelled by using linear Green functions, as shown by McCall (1994).

## 4 QUANTIFICATION OF SEISMICITY

To monitor rockmass response to mining one must be able to quantify continuously in time and space the parameters describing the flow changes in the stress and strain regime. From seismic observations, one can measure only that portion of stress, strain or rheological property of the rockmass associated with the radiation of recorded seismic waves.

### 4.1 Basic definitions

Seismicity, being the intermittent momentum flux due to the sudden motion of discrete lumps of rock, can be described by

the following four largely independent parameters:

- average time between events $\bar{t}$ ;
- average distance, _including source sizes, between consecutive events, $\bar{X}$ ;
- sum of seismic energies, $\Sigma E$;
- sum of seismic moments, $\Sigma M_{ij}$,

where averages and sums relate to the volume $\Delta V$ and time period $\Delta t$.

From these parameters one can calculate, for a given volume $\Delta V$ and time period $\Delta t$, the following parameters which statistically describe the physics of seismic flow of rock (Kostrov and Das, 1988; Mendecki, 1997).

*Seismic Strain Rate* [s$^{-1}$]

$$\dot{\varepsilon}_{s_{ij}}(\Delta V, \Delta t) = \frac{\Sigma M_{ij}}{2\mu\Delta V\Delta t} \tag{1}$$

where $\mu$ is rigidity. Seismic strain rate measures the rate of co-seismic inelastic deformation.

*Seismic Stress* [Pa]

$$\sigma_{s_{ij}}(\Delta V, \Delta t) = \frac{2\mu\Sigma E}{\Sigma M_{ij}} \tag{2}$$

Seismic stress measures stress changes due to seismicity.

*Seismic Viscosity* [Pa · s]

$$\eta_s(\Delta V, \Delta t) = \frac{\sigma_s}{\dot{\varepsilon}_s} = \frac{4\mu^2\Delta V\Delta t\Sigma E}{(\Sigma M_{ij})^2} \tag{3}$$

Seismic viscosity is similar to the fluid mechanics concept of turbulent or eddy viscosity. Unlike ordinary or molecular viscosity, turbulent viscosity does not describe the physical properties of the medium but characterises the statistical properties of the seismic deformation process. Lower seismic viscosity implies easier flow of seismic inelastic deformation or greater stress transfer due to seismicity.

*Seismic Relaxation Time* [s]

$$\tau_s(\Delta V, \Delta t) = \frac{\eta_s}{\mu} \tag{4}$$

Seismic relaxation time quantifies the rate of change of seismic stress during the seismic flow of rock and it separates the low frequency response from the high frequency response of the structure. It also defines the usefulness of the past data and the predictability of the flow of rock. The lower the relaxation time, the shorter the time span of useful past data and the less predictable the flow of rock.

*Seismic Deborah Number*

$$De_s(\Delta V, \Delta t) = \frac{\tau_s}{flowtime} \tag{5}$$

where *flowtime* is a design parameter not necessarily equal to $\Delta t$. Seismic Deborah number measures the ratio of elastic to

viscous forces in the seismic flow of rock and has successfully been used as a criterion to delineate volumes of rockmass softened by seismic activity (soft clusters).

*Seismic Diffusivity* [m$^2$/s]

The diffusivity is interpreted in terms of a characteristic distance of the process which varies only with the square root of time.

For a volume of linear dimension $L$ seismic diffusivity can be defined as

$$D_s(\Delta V, \Delta t) = \frac{L^2}{\tau_s} = \frac{(\Sigma M_{ij})^2}{4\mu L\Delta t\Sigma E} \tag{6}$$

Alternatively, one can define a more statistical version of seismic diffusivity as

$$d_s(\Delta V, \Delta t) = \frac{(\bar{X})^2}{\bar{t}} \tag{7}$$

where $\bar{X}$ may or may not include source sizes.

Seismic diffusivity can be used to quantify the magnitude, direction, velocity and acceleration of the migration of seismic activity and associated transfer of stresses in space and time.

*Seismic Schmidt Number*

$$Sc_s(\Delta V, \Delta t) = \frac{\eta_s}{\rho\, d_s} = \frac{4\mu^2\Delta V\Delta t(\bar{t})\Sigma E}{\rho\,(\bar{X})^2(\Sigma M)^2} \tag{8}$$

where $\rho$ is rock density. Seismic Schmidt number measures the degree of complexity in space and time (the degree of turbulence) of the seismic flow of rock. Note that seismic Schmidt number encompasses all four independent parameters describing seismicity: $\Sigma E, \Sigma M_{ij}, \bar{X}$, and $\bar{t}$.

4.2 Gradients and local clustering

Mining excavations create considerable gradients in stress, strain and their rates which the rockmass continuously reduces partly by means of elastic but mainly by inelastic deformation – rock flows towards openings or, in its phase space, it flows towards local equilibrium, reducing and transferring stresses. These processes are strongly time dependent i.e. the relaxation time changes over a few orders of magnitude, from seconds in the vicinity of the face just after blasting to years a few hundred metres away. Such strong spatial and temporal gradients are conducive to the development of large shear stresses which, if not diffused, may result in large and/or strong seismic events. One can analyze the gradients in seismic rockmass response to mining in a plane, in space or space-time (4D) by visual inspection of contour or isosurface plots and quantify them utilizing the definition of a gradient.

A local clustering of seismic activity in time and/or in space can relatively easily be accounted for when computing average values of different parameters quantifying seismicity. Let $\Omega$ represent the parameter of interest, say:

$$\Omega = \varepsilon_s, \sigma_s, \eta_s, \tau_s, D_s, Sc_s(\Delta V, \Delta t) \tag{9}$$

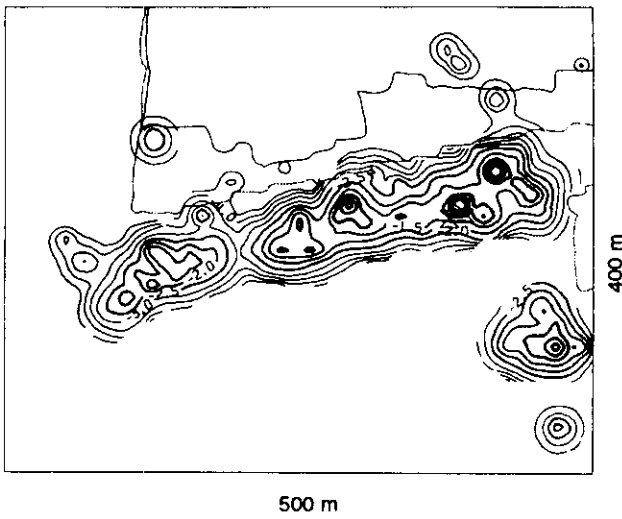then the local space and/or time clustering of $\Omega$ can be

**500 m**

Figure 7a   Contours of log$D_s$ of one month's data of seismic response to longwall mining in a South African gold mine. One can distinguish at least four areas of high gradient with $D_s$ as high as 0,5 to 1 m²/s. One of these areas attracted two larger seismic events, marked by the hourglass symbols, a day later.
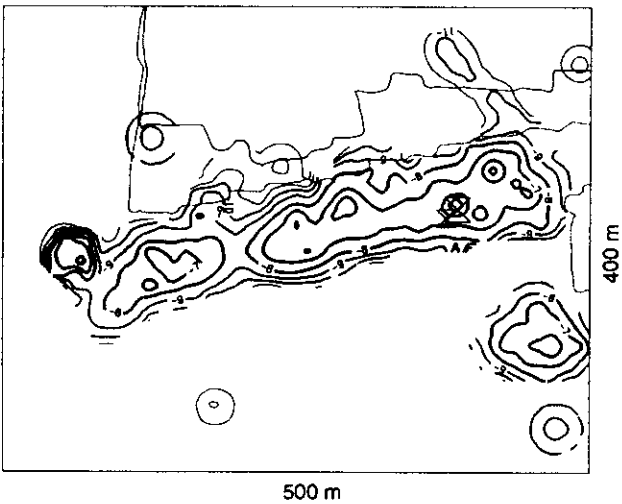


**500 m**

Figure 7b   Contours of $C(D_s;\bar{t}) = D_s/\bar{t}$ in [m²/s²], where seismic diffusivity, shown in Figure 7a, is divided by the local average time (over the grid size) between seismic events $\bar{t}$. The two larger events which subsequently occurred located in the area of the maximum $D_s/\bar{t}$.

expressed as

$$C(\Omega; \bar{X}, \bar{t}) = \frac{\Omega}{(\bar{X})(\bar{t})} \qquad (10)$$

where $\bar{X}$ and/or $\bar{t}$ would cater for the local space and/or temporal clustering of seismic activity. Equation 10 can be applied to contour or time history plots of different parameters.

Figures 7a and 7b show the results of backanalysis of the seismic rockmass response to mining which preceded the occurrence of two large seismic events during one day. Figure 7a shows contours of seismic diffusivity $D_s$ associated with mining a longwall for a period of one month in a South African gold mine. One can distinguish four areas of high gradient of diffusivity. Figure 7b shows contours of $D_s/\bar{t}$, where $\bar{t}$ is

taken over the grid size used for contouring. The area of maximum $D_s/\bar{t}$ attracted two seismic events of $m_M$=2.5 and $m_M$=2.0 a day later.

## 5. SEISMOLOGY FOR ROCKBURST PREDICTION

The following seismic behaviour has frequently been observed at some stage before rockmass instability in South African gold mines (Mendecki, 1997; van Aswegen et al., 1997).

* An overall softening, i.e. a decrease in the ratio of measured seismic energy $E$ of an event to the average energy radiated by events of the same moment in the area $\bar{E}(M)$ – called energy index $EI = E/\bar{E}(M)$ – or decrease in seismic viscosity ($\eta_s$) with time, spatially associated with seismic events close to the hypocentre of impending instability. The softened (fractured) zone is characterized by low seismic Deborah number. However, in a number of cases, short periods of increase and/or oscillations in these parameters just prior to instability have been reported

* An increase in the rate of coseismic deformation, as measured by the rate in cumulative source volume $V = M/\Delta\sigma$ or apparent volume $V_A = M/(2\sigma_A)$ plots, or by an increase in seismic diffusion $d_s$, due to the increase in seismic activity rate (decrease in $\bar{t}$) and/or, due to the softer nature of events occurring within the already fractured zone.

If softening coincides with accelerating deformation, then a decrease in seismic viscosity and an increase in seismic diffusion $d_s$ would result in a sharp decrease in seismic Schmidt number before instability.

Figure 8 shows an example of successful prediction of a magnitude 2.7 event associated with a dyke, which occurred on 24 April 1994. On 22 April an official warning was issued on the basis of observed accelerated seismic deformation and associated loss of stress, resulting in a considerable drop in seismic Schmidt number.

### 5.1 Time to failure

While considerable progress has been made in predicting larger, potentially damaging events in South African gold mines, it is still based on qualitative interpretation of quantitative data provided by the modern seismic systems. Note that at no stage before the event on April 24, (see Figure 8), was its imminence quantified, the timing of the warning was at the discretion of the mine seismologist. There is a need for a continuous quantitative interpretation of the potential for unstable rockmass behaviour so appropriate strategies can be developed to manage the risk. Very promising in this respect are recent developments in kinematics of failure, where imminence of potential instability can be quoted on the basis of seismic data.

According to this theory precursors should follow characteristic power laws where the rate of $\Omega$, being a seismic strain or other related measurable quantity, is proportional to the inverse power of the remaining time to failure

$$\frac{d\Omega}{dt} = \frac{k}{(t_f - t)^\alpha} \qquad (11)$$

where $k$ and $\alpha$ are constants and $t_f$ is time at failure. Integration
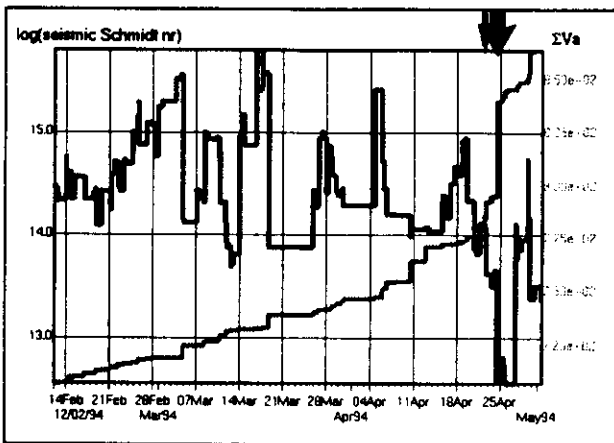
Figure 8 Time history of log(seismic Schmidt number), in black, and cumulative apparent volume ($\Sigma V_A$), in grey, for seismicity along the Postma dyke for the period 14/2/94 - 30/4/94. The grey arrow indicates the time of issue of a warning. The black arrow and the jump $\Sigma V_A$ show the time of occurrence of a local magnitude 2.7 tremor.
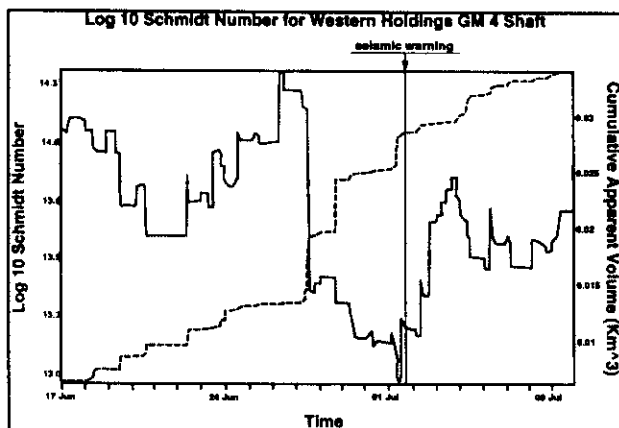


Figure 9 Due to the increase in the rate of cumulative apparent volume and the accompanying drop in seismic Schmidt number, a seismic warning was issued for the Western Holdings 4 Shaft pillar area on 1 July 1996. As a result of the warning, blasting was suspended for several days and consequently the seismic Schmidt number increased, the apparent volume levelled off and no damaging event occurred.

of equation (11) gives

$$\Omega(t) = A + B\,|(t_f - t)|^m \tag{12}$$

where $A$, $B$ are constants and $m = 1 - \alpha$, is a critical exponent which can be interpreted in terms of underlying fractal geometry.

This method has been in use in the prediction of materials failure, stability of slopes and earthquakes, e.g. Varnes and Bufe (1996) and has recently been applied to quantitative data supplied by the mine seismic networks (Mendecki, 1997).

Frequently observed oscillations in $\Omega$ of an increasing frequency as the failure approaches are part of the solution to time-to-failure equations with a complex exponent, where the imaginary part relates to discrete scale transformation and
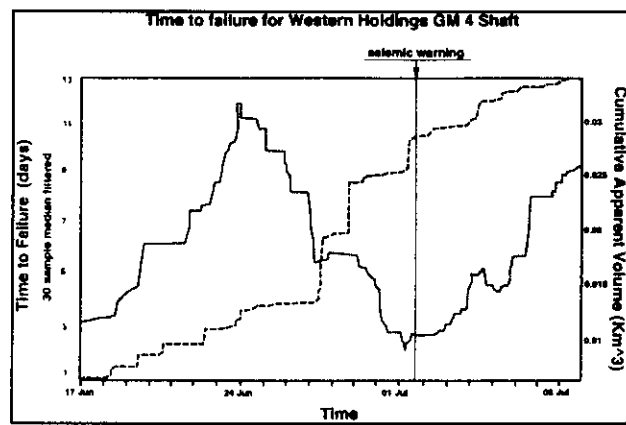


Figure 10 Time to failure for the case in Figure 9. As expected, time to failure drops with the seismic Schmidt number and increases after the action taken by the mine.

introduces log-periodic oscillations decorating the asymptotic power law (Sornette and Sammis, 1995; Saleur et al., 1996). The observed drop in seismic viscosity and thus seismic relaxation time of the complex spatially and temporally intermittent process of seismic deformation before failure could perhaps be one of the reasons for an increase in frequency response of the system.

As the observable quantity $\Omega$ one can use the cumulative apparent volume $\Sigma V_A$ or the inverse of the seismic Schmidt number, $1/Sc_r$, hopefully gaining sensitivity to precursory behaviour from a multidimensional description of seismic sources.

Figure 9 and Figure 10 show the behaviour of the seismic Schmidt number and time to failure derived from

$$\dot{\Omega} = \frac{\Sigma V_A}{(t)(EI)\Delta V} \tag{13}$$

for the Western Holdings 4 shaft pillar area, South Africa.

An official warning for the area was issued by the mine seismologist on 1 July 1996. As a result, blasting was suspended for several days. Mining resumed after that period and no major events were recorded. This case demonstrates an example of controlled mining where a 'success rate' of predicting strong seismic events may be lowered due to the early warnings and proactive measures, e.g. change in rate of mining or preconditioning, but makes mining safer.

6. CHAOS AND PREDICTABILITY OF SEISMIC ROCKMASS RESPONSE TO MINING

Chaos, at least at present, is rather a philosophical than a rigorous mathematical term (Brown and Chua, 1996). Chaos can be characterised as a deterministic means for generating randomness. Chaotic processes can be defined by algorithms whilst random processes cannot. Systems that exhibit chaotic behaviour do not admit an arbitrarily large horizon of predictability, i.e. the evolution of the dynamics underlying the processes cannot be known with acceptable accuracy for any increasingly large period of time. The presence of chaos signals, however, the causal type of evolution which indicates that future states depend on previous states in the physical

phase space. This means that, at least partly, attempts can be made to estimate future values of the observable that describes a chaotic process within finite, usually not large, ranges of time. These ranges of time are known as the limits of predictability. To determine the limits, one first needs to test for the deterministic nature of the process. In the event of a fully random case, no limits of predictability can be established. In such a case the statistical methods are the only tools one could use to 'guess' the future occurrences. An appropriate forecast – as opposed to guess – can be achieved in the case of deterministic systems. One of the most surprising ways of establishing the deterministic nature is to look for chaotic behaviour.

Various features of chaos, i.e. decaying autocorrelation functions, exponential loss of information and sensitive dependence on initial conditions, are independent characteristics of complex systems. The corresponding measure which quantifies the sensitivity to initial conditions is the Lyapunov exponent.

Assume that the phase space of the seismic response within a given time at a certain area has been delineated by either knowing the degrees of freedom which define the process or by embedding the time series of a significant physical parameter, e.g. the seismic moment (Radu et al., 1997). By embedding it is possible to obtain an attractor – the set of points in the phase-space visited by the solution to the evaluation equation – where the topological information will be preserved although the quantitative coordinates will differ (Takens, 1981; Sauer et al., 1991). Figure 11 displays a Poincaré surface of section through the reconstructed phase space using seismic moment as the embedding parameter. The appearance of an attractor, with its basin of attraction (lower density points) is clearly noticeable.

Now one can consider a trajectory in the phase space and a neighbouring trajectory with initial conditions $x$ and $x + \Delta x$, respectively. These trajectories will evolve in time yielding the tangent vector $\Delta x$ $(x,t)$ having the Euclidian norm $d$ $(x,t) = \|\Delta x$ $(x,t)\|$. The mean exponential rate of divergency $Ly$ of two initially close trajectories is defined as:

$$Ly(x,\Delta x) = \lim_{t \to \infty} \frac{1}{t} \log_2 \frac{d(x,t)}{d(x,0)}$$

$$d(x_0,0) \to 0$$

(14)

In an $N$- dimensional phase space there are $N$ such exponents. If at least one of them is positive, that means that the time series that led to the reconstruction of the phase space or simply the dynamics under study is chaotic. Given the finite nature of all possible measurements to date, the Lyapunov exponent can only be calculated for a given period of time (Wolf et al. 1985).

The second step in estimating the limits of predictability is to determine the information link $IL$ present in the time series of our measurements. The calculation of the autocorrelation function or the average mutual information are two options we can employ in order to calculate $IL$ which is in fact the delay used in the embedding of a time series (Abarbanel, 1990). $IL$ is determined as either the first zero of the autocorrelation function or the first minimum of the average mutual information. If the autocorrelation criterion is used the $IL$ signifies the number of consecutive events (measurements) in a time series that are correlated, in fact linearly dependent in a statistical way. If the average mutual information is used, $IL$
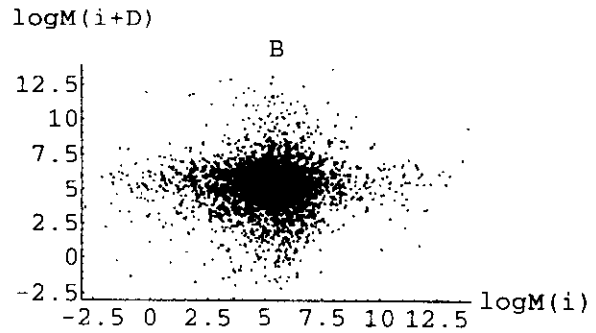


Figure 11    Poincaré map of the log$M$ attractor (after Radu et al. 1997).

quantifies the number of consecutive measurements (events) that are interrelated from an informative point of view.

Given the meaning of the Lyapunov exponent and the information link one can proceed to calculate the limit of predictability of a time series which contains for instance the history of a seismic parameter of interest $s = \{s_1, s_2, s_3,...,s_N\}$ where $N$ is the number of events recorded to date. When event $N+1$ occurs, the information link of the $N$th event will decrease from $IL$ by $Ly$. When the $N + 2$ event has occurred the information link will decrease further to $IL - 2Ly$. If, after the occurrence of the $N + k$ event, the information link between the $N$ event and the $k$th event, i.e. $IL - kLy$, is zero, the limit of predictability of the time series according to its current standing has been reached. This limit of predictability (expressed in number of events) is $IL/Ly$ and can be translated into a temporal limit if the correlation time of the series is known. Radu et al. (1997) estimated the limits of predictability of various seismic parameters for three areas in South African gold mines. They were finite and manageable ranging from a few hours to three weeks.

To gain some insight into the nature of the continuous seismic rockmass response to mining, a nonlinear time series analysis was performed on two very different types of waveforms. Figure 12 shows superimposed three-component waveforms of acceleration of a small 'well-behaved' seismic event recorded by five three-component stations and Figure 13 shows their autocorrelation functions calculated on the square root of the sum of the components.

Embedding, using the first zeroes of the respective autocorrelation functions as delays and subsequent calculations of the correlation dimensions from the correlation integral, (Grassberger and Procaccia, 1983; Radu et al., 1997), yielded the fractal dimensions of the attractors associated with the waveforms shown in Figure 12 – see Table 2.

The fact that the estimated correlation dimensions are all fractional indicates the chaotic behaviour of the waveforms, since strange attractors, i.e. attractors of fractal dimension, can only be exhibited by chaotic systems. The estimated correlation dimension tends to increase with the distance from the source or, rather, with the complexity of waveforms. This suggests that the propagation is deterministically chaotic. In addition, the calculated maximum Lyapunov exponents are all positive and increase with the complexity of the waveforms – see Table 2 for results. The low magnitude of the Lyapunov exponents

| Waveform No. | 1 | 2 | 3 | 4 | 5 |
|---|---|---|---|---|---|
| Embedding dimension (No. of points) | Correlation dimension | | | | |
| 3 (2388) | 2.82 | 2.79 | 2.84 | 2.96 | 2.92 |
| 4 (2388) | 3.32 | 3.55 | 3.68 | 3.67 | 3.84 |
| 5 (1988) | 3.40 | 3.63 | 3.71 | 3.79 | 3.92 |
| 6 (1588) | 3.38 | 3.52 | – | 3.73 | 3.92 |
| Estimated correlation dimension | 3.35 | 3.56 | 3.69 | 3.73 | 3.90 |
| Maximum Lyapunov exponent | 0.12 | 0.23 | 0.26 | 0.19 | 0.46 |

Table 2. Correlation dimension versus embedding dimension and Lyapunov exponents for five waveforms generated by a 'well-behaved' event.
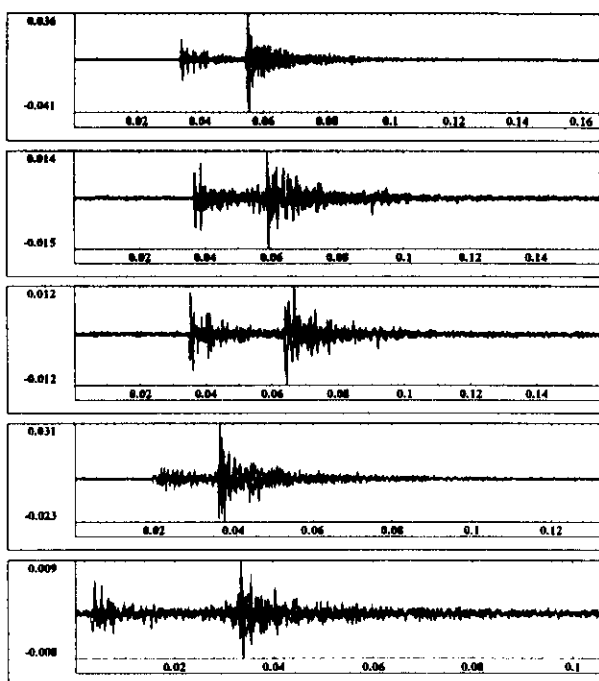




Figure 12 Superimposed three-component waveforms of acceleration of a 'well-behaved' seismic event of $m_M$=-2.5 recorded by five stations while monitoring the progress of a caving operation at Northparks, New South Wales, Australia. The hypocentral distances vary between 130 and 300 m.

Figure 13 Autocorrelation function of the waveforms shown in Figure 12. The first zero, marked by a circle, signifies the timespan over which the data is correlated linearly and was used as the delay in the embedding procedure.
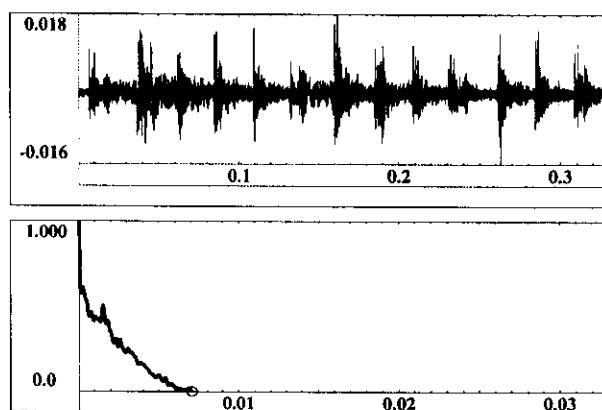


Figure 14 Superimposed three-component waveform of acceleration and its autocorrelation function of a complex event associated with blasting recorded at Northparks, New South Wales, Australia.

indicates the weak chaos in the analyzed waveforms. Figure 14 shows waveforms and the autocorrelation function of a complex event associated with blasts, i.e. seismic rockmass response to blasting. In this case the estimated correlation dimension on 4988 measured points is 5.2 and the maximum Lyapunov exponent 0.27, which indicates higher dimensional dynamics but not necessarily more chaotic behaviour.

The calculations of the correlation dimension should still be carefully verified, specifically with surrogate waveforms, i.e. reprocessed waveforms which have the same Fourier power spectrum but have lost all of their deterministic characteristics (Theiler et al., 1992). Nevertheless, the results are similar to those obtained by Corrieg and Urquizu (1996), for S coda waves of local events in the Pyrenees where correlation dimensions varied between 3.43 and 3.94. The Lyapunov exponents are lower in this study probably due to the lower complexity of the waveforms imposed by the propagation over relatively short distances.

While the presented results are of a preliminary nature, they indicate that seismic rockmass response to mining is chaotic deterministic with limited but manageable predictability, whether measured intermittently – seismicity – or continuously – ground motion. In such cases, the methods of nonlinear dynamics may offer an additional insight into the complex processes associated with seismic rockmass response to mining.

## 7. FINAL COMMENTS

The following comments on future research and development needs are offered to realize the stated objectives of monitoring seismic rockmass response to mining.

1 One needs to increase the sensitivity i.e. the frequency range, amplitude range and the throughput of seismic monitoring systems, to account for a greater portion of stress and strain changes due to mining and to gain information from the parts of the rockmass otherwise considered inactive and from the periods of time otherwise considered quiet.

2 There is a need to reliably describe the source of a seismic event not only by its time, location(s), radiated seismic energy, seismic moment, and size but in addition by its shape, orientation and duration, and to quantify seismicity by parameters pertaining to changes in stress, strain and rheology of seismic deformation processes. Such a quantification will facilitate the integration of results of seismic monitoring and numerical modelling. Assumptions and results of numerical 'stress' modelling, which is the most important design tool, need to be verified with quantified observations to maintain credibility. For this reason, developers of numerical models should apply a manageable number of meaningful, measurable parameters to models which are used as design tools.

3 Tangible, although not yet satisfactory, progress has been achieved in forward prediction of rockbursts in South African gold mines. In most cases, the predictions are done on the basis of qualitative interpretation of quantitative data provided by modern seismic systems i.e. accelerating seismic deformation and/or loss of stress. The recent development in 'time-to-failure' provides a unique opportunity not only to quantify the imminence of potential instability and to make the prediction process more objective, but also to correlate with and eventually to integrate this type of development into numerical modelling.

4 Looking at Figure 1, it is obvious that by analysing only 'good quality' waveforms of 'well behaved' seismic events one is utilising only a fraction of the time rockmass responds to mining seismically. In the case of 1000 seismic

events recorded and analysed per day of an average duration say 0.1 s each, one is effectively 'listening' to the rockmass for only 100/86400 = 0.1% of the day. Surely there is useful information lost during the remaining 99.9% of the time, since there are numerous coherent structures associated with convolved fracturing, unprocessable larger events and nonstochastic noise that constitutes a legitimate seismic rockmass response to mining.

Since the rockmass response to mining is a nonlinear, dissipative system which exhibits a chaotic behaviour, one can not ignore even small – not to mention macro – fluctuations since they contain important qualitative information about the system and can alter its behaviour in a fundamental way.

In non-chaotic deterministic systems nothing interesting happens, late developments are similar to those at an early stage. On the other hand, in highly chaotic systems, history is obscured very quickly, e.g. rockmass response to blasting where the rockmass quickly forgets its past and the information about its behaviour in the near future is largely encoded in its response during the few hours after the blasts.

It is therefore important to develop a system for *continuous*, in addition to intermittent, monitoring of seismic rockmass response to mining, where sensors are positioned at the centre of the volume of interest *where the action is*, as opposed to being outside in the far field. The processing and analyses can utilise the methods of nonlinear dynamics where invariants, or classifiers of the motion, i.e. fractal dimensions and local, or finite time, Lyapunov exponents, are computed in the reconstructed phase space from recorded ground motion.

One can then build a forecasting model for the dynamics to predict forward in time from any new initial condition close to or on the attractor within the limits of the intrinsic instabilities embodied in the positive Lyapunov exponent. Alternatively, given a set of experimental chaotic data and a set of model differential equations, one can invert the numerical values for these parameters and thus test the model against the data (Baker et al., 1996). The next step, or rather, opportunity, is to use chaos in an attempt to control (stabilize) or decontrol (destabilize or trigger) the systems in a determined fashion at the right time so the chaos present in the system will do most of the work. The phase space structure of a chaotic system contains many simpler unstable topological features through which the system has passed driven by mining parameters i.e. rate and type of blasting or extraction, mine layout etc). Thus, the careful adjustment of these same parameters using the known stable and unstable directions of the vector field may allow one to stabilise what has become unstable or vice versa, e.g. Abarbanel (1996); Hu et al. (1995); Chen and Lai (1996); Paskota (1996); Chen and Dong (1993a); Chen and Dong (1993b); Jackson (1991); Shinbrot el al. (1993). While extremely attractive, the idea of controlled manipulation of the rockmass response to mining into a desirable state of stability or instability seems difficult – but then:

> *all things are difficult*
> *until they are easy.*

## Acknowledgements

## References

Abarbanel, H D I, Brown, R and Kadtke, J B (1990). Prediction in chaotic nonlinear systems: Methods for time series with broadband Fourier spectra. *Physical Review*, A41, 1782-1807.

Abarbanel, H D I (1996). *Analysis of Observed Chaotic Data*. Institute for Nonlinear Science. Springer-Verlag.

Baker, G L, Gollub, J P and Blackburn, J A (1996). Inverting chaos: extracting system parameters from experimental data. *Chaos*, 6, 4, 528-533.

Beresnev, I A and Wen, K-L (1996). The possibility of observing nonlinear path effect in earthquake-induced seismic wave propagation. *Bull. Seism. Soc. Am.*, 86, 4, 1028-1041.

Brown, R and Chua, L O (1996). Clarifying chaos; examples and contre-examples, *Int. J. Bifurcation and Chaos*, 6, 3, 219-249.

Cichocki, A and Unbehauen, R (1993). *Neural Networks for Optimization and Signal Processing*. John Wiley and Sons, New York.

Cao, S and Greenhalgh, S (1994). Finite-difference solution of the eikonal equation using an efficient, first-arrival, wavefront tracking scheme. *Geophysics*, 59, 632-643.

Chen, G and Lai, D (1996). Feedback control of Lyapunov exponents for discrete-time dynamical systems. *Int. J. Bifurcation and Chaos*, 6, 7, 1341-1349.

Chen, G and Dong, X (1993a). From chaos to order — Perspectives and methodologies in controlling chaotic nonlinear dynamical systems. *Int. J. Bifurcation and Chaos*, 3, 1363-1410.

Chen, G and Dong, X (1993b). Control of chaos — A survey. *Proc. 32nd Contr. Decis. Conf.*, San Antonia, TX, 469-474.

Corrieg, A M and Urquizu, M (1996). Chaotic behaviour of coda waves in the eastern Pyrenees. *Geophys. J. Int.*, 126, 113-122.

Dziewonski, A M and Woodhouse, J H (1982) Studies of seismic source using normal-mode theory. In: *Earthquakes: Observation, Theory and Interpretation*. Kanamori & Boschi (eds.) North-Holland Publishing Company. 45-138.

Dzhafarov, A H (1997a). Deconvolution, polarization and wavelet transform of seismic signals. In: *Seismic Monitoring in Mines*, Mendecki A J (ed), Chapman and Hall, London. 41-66.

Dzhafarov, A H (1997b). Seismic raytracing. In: *Seismic Monitoring in Mines*, Mendecki, A J (ed), Chapman and Hall, London. 67-86.

Gibowicz, S J and Kijko, A (1994). *An Introduction to Mining Seismology*. Academic Press, New York.

Grassberger, P and Procaccia, I (1983). Characterisation of strange attractors. *Phys. Rev. Letters*, 50, 346-349.

Jackson, E A (1991). On the control of complex dynamic systems. *Physica*, D50, 341-366.

Jech, J (1989). Seismic tomography in the Ostrava-Karvina mining region. In: *Seismicity in Mines*, (Gibowicz, S J, ed.). Special Issue, *Pure Appl. Geophys.*, 129, 597-608.

Hu, G, Qu, Z and He, K (1995). Feedback control of chaos in spatiotemporal systems. *Int. J. Bifurcation and chaos*, 5, 4, 901-936.

Kostrov, B V and Das, S (1988). *Principles of Earthquake Source Mechanics*. Cambridge University Press, Cambridge.

Maxwell, S C and Young, R P (1993). Associations between temporal velocity changes and induced seismicity, *Geophys. Res. Lett.*, 20, 2929-2932.

Maxwell, S C and Young, R P (1997). Seismic velocity inversion from microseismic data. In: *Seismic Monitoring in Mines*, Mendecki A J (ed), Chapman and Hall, London. 108-118.

McCall K R (1994). Theoretical study of nonlinear elastic wave propagation. *J. Geophys. Res.*, 99, 2591-2600.

Mendecki, A J (1987). Rockmass anisotropy modelling by inversion of mine tremor data. In: *Proceedings of 6th International Congress on Rock Mechanics*, (Herget, G and Vongpaisal, S, eds.), Balkema, Rotterdam, 1141-1144.

Mendecki, A J (1993). Real time quantitative seismology in mines. Keynote lecture. In: *Proceedings of the 3rd International Symposium on Rockburst and Seismicity in Mines* (Young, R P, ed.), Kingston, Canada. Balkema, Rotterdam, 287-296.

Mendecki, A J (1997). Quantitative seismology and rock mass stability. In: *Seismic Monitoring in Mines*, Mendecki A J (ed), Chapman and Hall, London. 178-218.

Mendecki, A J and Niewiadomski, J (1997). Spectral analysis and seismic source parameters. In: *Seismic Monitoring in Mines*, Mendecki A J (ed), Chapman and Hall, London. 144-158.

Mendecki, A J and Sciocatti, M (1997). Location of seismic events. In: *Seismic Monitoring in Mines*, Mendecki A J (ed), Chapman and Hall, London. 87-107.

Milev, A M, Spottiswoode, S M and Stewart, R D (in prep.) Automatic location of seismic event multiplets by crosscorrelation criteria. Submitted *Bull. Seism. Soc. Am.* (1996).

Moser, T J and Pajchel, J (1996). Recessive seismic ray modelling: applications in inversion and VSP. Submitted to Geophysical Prospecting.

Mountfort, P and Mendecki, A J (1997). Seismic monitoring systems. In: *Seismic Monitoring in Mines*, Mendecki A J (ed), Chapman and Hall, London. 21-40.

Niewiadomski, J (1997). Seismic source and moment tensor in the time domain. In: *Seismic Monitoring in Mines*, Mendecki A J (ed), Chapman and Hall, London. 119-143.

Oh, E (1996). Development of a computer-based calibration facility for low-frequency acoustic emission transducers. In: *Procceedings of 6th Acoustic Emission/Microseismic Activity in Geological Structures and Materials Conference*, Pennsylvania State University (H.R. Hardy ed.). Trans Tech

Publications, Clausthal-Zellerfield.

Park, J, Lindberg, C R and Vernon, F L (1987). Multitaper spectral analysis of high-frequency seismograms. *J. Geophys. Res.*, **92**, B12, 12675–12684.

Paskota, M (1996). On local control of chaos: The neighbourhood size. *Int. J. Bifurcation and Chaos*, **6**, 169–178.

Poupinet, G, Ellsworth W L and Frechet, J (1984). Monitoring velocity variations in the crust using earthquake doublets: an application to the Calaveras fault, California, *J. Geophys. Res.*, **89**, 5719–5731.

Qin, F, Luo, Y, Olsen, K B, Cai, W and Schuster, G T (1992). Finite-difference solution of the eikonal equation along expanding wavefronts, *Geophysics*, **57**, 479–487.

Radu, S, Sciocatti, M and Mendecki, A J (1997). Nonlinear dynamics of seismic flow of rock. In: *Seismic Monitoring in Mines*, Mendecki A J (ed), Chapman and Hall, London.

Saleur, H, Sammis, C G, and Sornette, D (1996). Discrete scale invariance, complex fractal dimensions, and log-periodic fluctuations in seismicity. *J. Geophys. Res.*, **101**, B8, 17661–17677.

Sauer, T, Yorke, A and Casdagli, M (1991). Embedology. *J. Stat. Phys.*, **65**, 579–616.

Shinbrot, T, Grebozi, C, Otto, E, and Yorke, J A (1993). Using small perturbation to control chaos. *Nature*, **363**, 411–417.

Šíleny, J and Pšenčík, I (1995). Mechanisms of local earthquakes in 3D inhomogeneous media determined by waveform inversion. *Geophys. J. Int.*, **121**, 459–479.

Sornette, D and Sammis, C G (1995). Complex critical exponents from renormalisation group theory of earthquakes: implications for earthquake predictions. *J. Phys. I. France*, **5**, 607–619.

Spence, W (1980). Relative epicenter determination using P wave arrival-time differences. *Bull. Seism. Soc. Am.*, **70**, 171–183.

Spottiswoode, S M (1993). Seismic attenuation in deep level mines. In: *Proceedings of the 3rd International Symposium on Rockburst and Seismicity in Mines*, (R P Young, ed.), Kingston, Canada. Balkema, Rotterdam, 409–414.

Takens, F (1981). Detecting strange attractors in turbulence. In: *Lecture Notes in Mathematics*. (Rand, D A and Young, L S, eds.) Springer, Berlin, 366–381.

Theiler, J, Galdrikian, B, Longtin, A, Eubank, S and Doyne Farmer, J (1992). Using surrogate data to detect nonlinearity in time series. In: *Nonlinear Modelling and Forecasting, SFI studies in the Sciences of Complexity, Proc. XII*, (Casdagli, M and Eubank, S eds.) 163–188. Addison-Wesley.

Urbancic, T I, Trifu, C I , Mercer, R A, Feustal, A J and Alexander, J A G (1996). Automatic time-domain calculation of source parameters for the analysis of induced seismicity. *Bull. Seism. Soc. Am.*, **86**, 5, 1627–1633.

van Aswegen, G, Mendecki, A J and Funk, C (1997). Application of quantitative seismology in mines. In: *Seismic Monitoring in Mines*, Mendecki, A J (ed), Chapman and Hall, London. 220–245.

Varnes D J and Bufe C J (1996) The cyclic and fractal seismic series preceding an $m_b$ 4.8 earthquake on 1980 February 14 near the Virgin Islands, *Geophys. J. Int.*, **124**, 149–158.

Vidale, J (1990). Finite-difference calculation of traveltimes in 3D. *Geophysics*, **55**, 521–526.

Vinje, V, Iversen, E, Gjoystadl, H and Astebøl, K (1993). Estimation of multivalued arrivals in 3D models using wavefront construction. In: *Extended abstracts of the 63rd annual SEG meeting and Exposition*. Washington DC, SEG. 1157–1166.

Wolf, A, Swift, J B, Swinney, H L and Vastano, J (1985). Determining Lyapunov exponents from a time series. *Physica D*, **16**, 285–317.
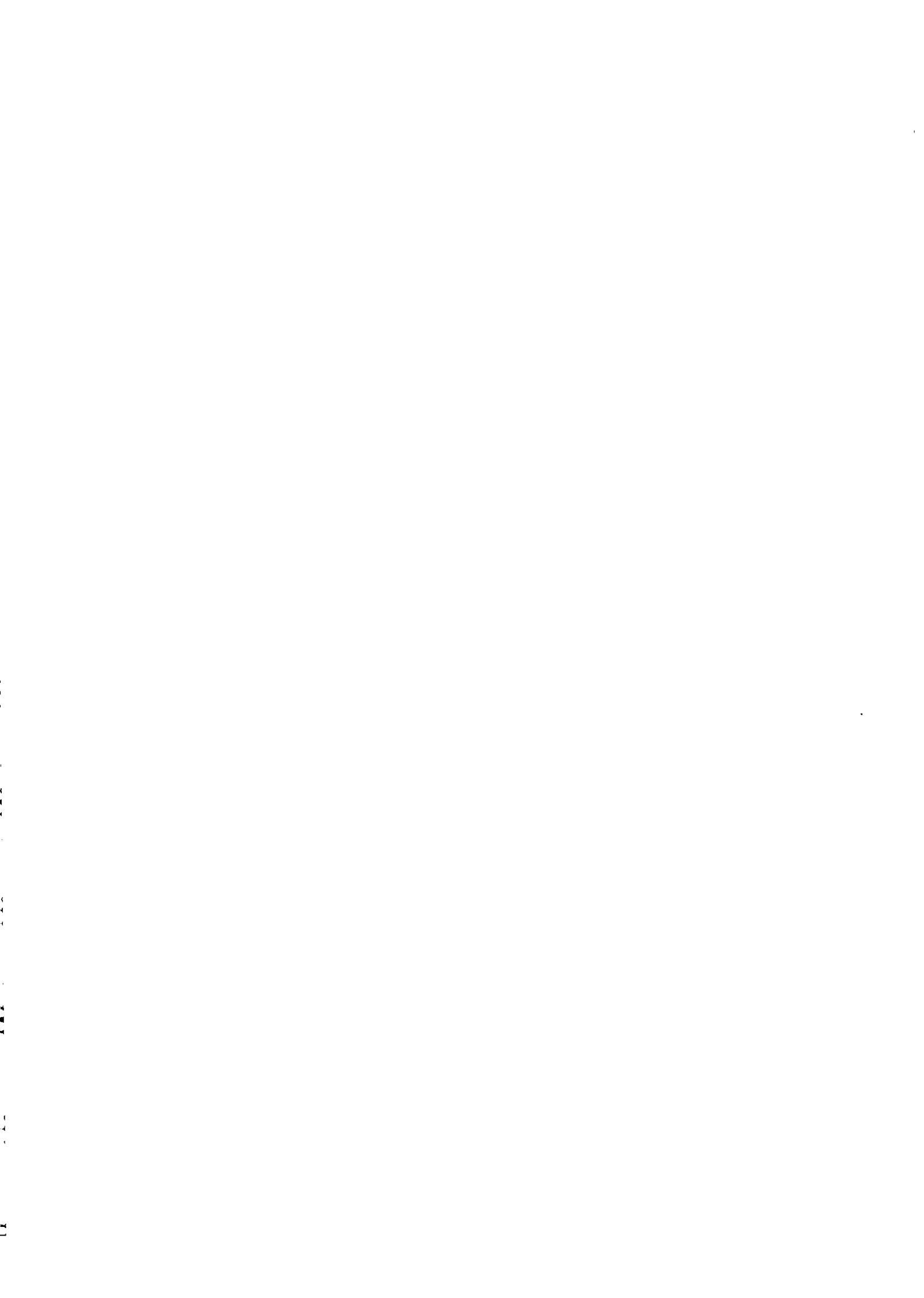
# Seismic Monitoring in Mines

Edited by

# Dr A.J. Mendecki

*Managing Director and Head of Research at ISS International,*
*Welkom, South Africa*

**CHAPMAN & HALL**

London · Weinheim · New York · Tokyo · Melbourne · Madras

# Contents

# Contributors

Dr A.H. Dzhafarov
ISS International, South Africa

Mr C. Funk
ISS International, South Africa

Dr S.C. Maxwell
Department of Geophysics, Keele University, UK

Dr A.J. Mendecki
ISS International, South Africa

Dr P. Mountfort
ISS International, South Africa

Dr J. Niewiadomski
ISS International, South Africa

Dr S. Radu
ISS International, South Africa

Mr M. Sciocatti
ISS International, South Africa

Dr G. van Aswegen
ISS International, South Africa

Prof R.P. Young
Department of Geophysics, Keele University, UK

# Preface

Routine seismic monitoring in mines was introduced over 30 years ago with two main objectives in mind:

- immediate location of larger seismic events to guide rescue operations;
- prediction of large rockmass instabilities.

The first objective was achieved fairly quickly, but with the subsequent development of mine communication systems, its strategic importance has diminished. The very limited success with prediction can, at least partially, be attributed to three factors:

- seismic monitoring systems based on analogue technology that provided noisy and, frequently, poorly calibrated data of limited dynamic range;
- the non-quantitative description of a seismic event by at best its local magnitude; and
- the resultant non-quantitative analysis of seismicity, frequently through parameters of some statistical distributions, with a somewhat loose but imaginative physical interpretation.

The introduction of modern digital seismic systems to mines and progress in the theory and methods of quantitative seismology have enabled the implementation of realtime seismic monitoring as a management tool, quantifying rockmass response to mining and achieving the first tangible results with prediction.

A seismic event, being a sudden inelastic deformation within the rockmass, can now routinely be quantified in terms of seismic moment, its tensor, and radiated seismic energy, so that the overall size of, and stress released at, the seismic source can be estimated.

Thus seismicity, being the intermittent momentum flux due to the sudden motion of discrete lumps of rock, and its associated stress and strain changes in the rock, can be quantified. This brings seismology into the realms of rock mechanics and rheology, where changes in stress, strain rate, flow viscosity and diffusion are fundamental in determining the stability of the deforming

structures.

However, from seismological observation one can only measure that portion of stress, strain or rheology of the process which is associated with recorded seismic waves. The wider the frequency and amplitude range, and the higher the throughput, of the seismic monitoring system, the more reliable and more relevant the measured values of these parameters become.

The objectives of seismic monitoring in mines then become:

- to verify the parameters and assumptions of mine design while mining;
- to predict larger instabilities;
- to backanalyse, so that we learn from history.

Seismic monitoring in mines consists of sensors, data acquisition, signal processing, seismological analysis, quantification of the seismic response of the rockmass to mining, and finally, interpretation in terms of the potential for instability. Since each of these stages must be conducted with great care for meaningful results, this book has been structured accordingly.

The principal objective of the book is to suggest, but not prescribe, possible solutions to the problems encountered in achieving the above objectives and to show examples of successful applications. No claim is made for completeness. The emphasis has clearly been placed on parameters describing seismic sources as opposed to changes in wave velocity or attenuation to infer the state of the rockmass. Nevertheless, we hope all users of mine seismic systems will be inspired to gain more insight from their data and increase the value of their systems as management tools.

Aleksander J. Mendecki, Editor.

# Acknowledgements